RXTE and *BeppoSAX* Observations of the Transient X-ray Pulsar XTE J1859+083

R. H. D. Corbet[1,2], J.J.M. in 't Zand[3], A.M. Levine[4], F.E. Marshall[2]

ABSTRACT

We present observations of the 9.8 s X-ray pulsar XTE J1859+083 made with the All-Sky Monitor (ASM) and Proportional Counter Array (PCA) on board the *Rossi X-ray Timing Explorer* (*RXTE*), and the Wide Field Cameras (WFC) on board *BeppoSAX*. The ASM data cover a 12 year time interval and show that an extended outburst occurred between approximately MJD 50,250 and 50,460 (1996 June 16 to 1997 January 12). The ASM data excluding this outburst interval suggest a possible 61 day modulation. Eighteen sets of PCA observations were obtained over an approximately one month interval in 1999. The flux variability measured with the PCA appears consistent with the possible period found with the ASM. The PCA measurements of the pulse period showed it to decrease non-monotonically and then to increase significantly. Doppler shifts due to orbital motion rather than accretion torques appear to be better able to explain the pulse period changes. Observations with the WFC during the extended outburst give an error box which is consistent with a previously determined PCA error box but is significantly smaller. The transient nature of XTE J1859+083 and the length of its pulse period are consistent with it being a Be/neutron star binary. The possible 61 day orbital period would be of the expected length for a Be star system with a 9.8 s pulse period.

Subject headings: stars: individual (XTE J1859+083) — stars: neutron — X-rays: binaries

---

[1]University of Maryland, Baltimore County; corbet@umbc.edu

[2]Astrophysics Science Division, Mail Code 662, NASA Goddard Space Flight Center, Greenbelt, MD 20771

[3]SRON Netherlands Institute for Space Research, Sorbonnelaan 2, 3584 CA Utrecht, The Netherlands jeanz@sron.nl; Astronomical Institute, Utrecht University, PO Box 80000, 3508 TA Utrecht, The Netherlands

[4]Kavli Institute for Astrophysics and Space Research, MIT, Cambridge, MA 02139

1. Introduction

The X-ray source XTE J1859+083 was discovered by Marshall et al. (1999) in observations made with the *Rossi X-ray Timing Explorer* (*RXTE*) Proportional Counter Array (PCA) on 1999 August 8 (MJD 51,398) during slews between pointed observations of other targets. Although it was not possible to search for pulsations in the slew observation, Marshall et al. (1999) found pulsations at a period of 9.801 ± 0.002 s in an observation made on 1999 August 16. Cross-scan observations with the PCA reported by Marshall et al. (1999) located the source at R.A. = $18^h59.1^m$, decl. = +8° 15' (equinox 2000.0), with an estimated uncertainty of 2' (90% confidence).

Since the discovery of this source, the only other observations of XTE J1859+083 that have been reported are by Romano et al. (2007) who observed the PCA position on 2007 November 16 to 17 with the *Swift* X-ray Telescope. Romano et al. (2007) did not detect the source and reported an upper limit of 5×10^{-14} ergs cm^{-2} s^{-1} in the energy range of 0.3 to 10 keV.

The transient nature of XTE J1859+083 and its pulsations suggest that it might be a member of the Be/neutron star binary class of objects (e.g., Charles & Coe 2006). We present here the results of additional observations with the *RXTE* PCA, an improved position from *BeppoSAX* Wide Field Camera (WFC) observations, and an analysis of the *RXTE* All Sky Monitor (ASM) light curve which reveals a possible orbital period. The results of the observations are all consistent with a Be/neutron star classification.

2. Observations

2.1. *RXTE* PCA

The PCA is described in detail by Jahoda et al. (1996, 2006). This instrument consists of five nearly identical Proportional Counter Units (PCUs) sensitive to X-rays with energies between 2 and 60 keV with a total effective area of 6500 cm^2. The Crab produces 13,000 counts s^{-1} for the entire PCA across the complete energy band. The PCA spectral resolution at 6 keV is approximately 18%, and the field of view is 1° FWHM.

The first PCA detection of XTE J1859+083 by Marshall et al. (1999) occurred serendipitously during a slew between other targets. Subsequent to that, pointed observations were carried out with two sets of observations being made every few days over a period of about 38 days. The log of PCA observations is given in Table **??**.

We analyzed the *RXTE* PCA observations using standard procedures for background subtraction and light curve and spectrum extraction. In Table **??** we give the fluxes resulting from fitting the spectra obtained from each observation with the typical X-ray pulsar model of an absorbed power-law with a high-energy cutoff (White et al. 1983). This model gave a good fit for all observations and we see no large change in spectral parameters as the flux declines with only possibly a small amount of steepening of the spectral slope at lower fluxes. The mean spectral parameters are found to be: photon index = 0.84 ± 0.03, $N_{\rm H}$ = 2.1 ± 0.2 × 10^{22} cm^{-2}, $E_{\rm cut}$ = 6.41 ± 0.06 keV, and $E_{\rm fold}$ = 13.0 ± 0.3 keV.

We also performed a timing analysis of the standard mode 1 data which have a time resolution of 0.125 s. Combining different observations within a given day typically gives excellent measurements. For a few observations it was not possible to obtain an unambiguous phase-connected solution. The pulse timing results are given in Table **??** and plotted in Fig. **??**. The period is found to change during the observations with an initial decreasing trend in which the period changes are not monotonic followed by a period increase revealed by a single period measurement. The flux from XTE J1859+083 is seen to initially decline followed by a low amplitude rebrightening at ∼MJD 51,432.

2.2. *RXTE* ASM

The *RXTE* ASM (Levine et al. 1996) consists of three similar Scanning Shadow Cameras which perform sets of 90 second pointed observations ("dwells") so as to cover ∼80% of the sky every ∼90 minutes. Light curves are available in three energy bands: 1.5 to 3 keV, 3 to 5 keV, and 5 to 12 keV. Source intensities are quoted as the count rates expected if the source was in the center of the field of view of Scanning Shadow Camera 1 in March 1996. With this convention, the Crab Nebula has an intensity of 75.5 counts s^{-1} over the 1.5 - 12 keV energy range and intensities of 26.8 (1.5 - 3 keV), 23.3 (3 - 5 keV), and 25.4 (5 - 12 keV) counts s^{-1} in each individual band. Observations of blank field regions away from the Galactic center suggest that background subtraction may produce a systematic uncertainty of about 0.1 counts s^{-1} (Remillard & Levine 1997). The ASM light curves used in our analysis span the period from MJD 50,088 to 54,573 (1996 January 6 to 2008 April 17).

The ASM light curve of XTE J1859+083 is plotted in Fig. **??**. The light curve shows that an extended outburst occurred between approximately MJD 50,250 to 50,460. If this source is a Be star system, as suggested by Romano et al. (2007), then such a long duration event is likely to be a "Type II" outburst during which periodic modulation is not expected to be present (e.g. Stella et al. 1986). We used power spectra of the light curves to search for periodic modulation and in all cases the calculation of power spectra employed the "semi-

weighting" scheme discussed in Corbet et al. (2007a, b). The power spectrum of the entire light curve (Fig. **??**) is dominated by low frequency noise due to the extended outburst. However, the power spectrum of just the ASM light curve obtained since MJD 50,460, after the end of the outburst, shows a peak near a period of 60.6 days (Fig. **??**). The nominal false alarm probability (FAP) of obtaining a peak with this strength or greater in the total frequency range considered is approximately 1%. However, for the FAP to be completely valid the number of independent trials, i.e. the frequency range considered, must be decided before a period is searched for (e.g. Scargle 1982). The nominal significance calculation also does not take into account the difficult to quantify decision to exclude part of the data and that the peak was first noted while searching through ASM light curves of many sources and not just XTE J1859+083. Therefore, the significance of the peak at 60.6 days is <99% and an exact figure cannot be given. We also calculated power spectra of the light curves in the 3 ASM energy bands. None of these power spectra showed a modulation near 60 days that was more significant than for the full energy range. In order to further quantify the possible periodic modulation we fitted a sine wave to the light curve since MJD 50,460. This gave a period of 60.65 ± 0.08 days with epoch of maximum flux occurring at MJD 52,549.1 ± 1.5. The fitted full amplitude of the modulation is 0.12 ± 0.02 counts s^{-1}, equivalent to approximately 1.6 mCrab, although the folded light curve shows a somewhat higher peak count rate (Fig. **??**).

2.3. *BeppoSAX* WFC

The *BeppoSAX* WFC instrument and its observing program are described by Jager et al. (1997) and Verrecchia et al. (2007) respectively. The WFCs were two identical coded mask instruments operating in the range 1.8 - 28 keV. The FOV was 40° by 40° with a FWHM angular resolution of 5'. The source location accuracy for bright sources in crowded fields was 0.7' at 99% confidence level, and larger for sources detected at lower significance levels. The on-axis sensitivity was between 2 to 10 mCrab for a typical *BeppoSAX* WFC observation of 3×10^4 s, and depended on the intensities of other sources in the same FOV. The WFCs pointed in opposite directions from each other and also at 90° from the Narrow Field Instruments also on board *BeppoSAX*. The WFCs operated between 1996 April 30 (MJD 50,203) and 2002 April 30 (MJD 52,394) and covered the entire sky multiple times.

We searched for the combination of images that produced the most significant detection of XTE J1859+083. It was found that data taken between MJD 50,340.65 and 50,395.91, i.e. during the period when the ASM light curve indicates that XTE J1859+083 was in an extended outburst, gave the best results, and the signal-to-noise ratio is 16.7 for this

interval. The best-fit coordinates are: 18^h 59^m 2.4^s, +8° 13' 57" (equinox 2000.0). with a 99% confidence error radius of 1.6′. For a Gaussian error distribution this translates to a 1.0′ radius at a 90% confidence level. This WFC error region has a four times smaller area than the previously determined PCA position. Outside this interval we found no significant detection of XTE J1859+083. The equivalent Galactic coordinates are $l = 41.12°$, $b = 2.07°$.

We plot both the PCA and WFC error regions on red and blue Digitized Sky Survey images in Fig. **??**. The DSS images are reported to be complete down to $V = 21$ (Monet et al. 2003). Several stars are visible in the overlap of the error boxes and the brightest object is USNO-B1.0 0982-0467446 ($B = 14.7$)/2MASS 18590277+0814220 ($I = 11.7$). However, despite the reduction in the size of the error box, without additional information on the objects in the error box we cannot yet determine the optical counterpart.

3. Discussion

A 60.6 day period is consistent with the orbital period expected for a Be star system containing a 9.8 s X-ray pulsar (Corbet 1986). However, the period is of modest significance in the power spectrum. We therefore investigate whether the PCA pulse timing and flux measurements can help determine whether this is the orbital period of the system.

We first consider whether the changes in the pulse period could be caused by accretion torques or orbital Doppler shifts. If the initial period decrease was caused by accretion torques, it requires a luminosity of about 10^{39} ergs s^{-1} (Joss & Rappaport 1984). However, the brightest flux seen with the PCA only corresponds to about 10^{36} ergs s^{-1} at 10 kpc. Period change primarily caused by accretion torques thus appears to be unlikely.

The mass function of a binary is given by $f(M) = P_{orb}K^3(1-e)^{3/2}/2\pi G$. This corresponds to the minimum mass of the primary star. We can estimate the mass function of XTE J1859+083 for the assumptions that the orbital period is 61 days and that the observed pulse period changes are due to orbital motion. Assuming a circular orbit for simplicity, the observed maximum and minimum pulse periods imply a velocity semi-amplitude of $\gtrsim 100$ km s^{-1} which implies a mass function of $\gtrsim 6$ $M_\odot$. The orbit is not fully sampled which suggests the velocity amplitude should be larger than implied by the limited pulse period measurements, and hence that the mass function would be larger. Conversely, if the orbit is significantly eccentric, as is common for some Be star systems, then the mass function could be smaller. Nevertheless, it appears that it is not unrealistic to account for the observed pulse period changes by orbital Doppler motion. It is thus probable that orbital Doppler shifts were more important than accretion torques in producing the observed pulse period

changes.

We next consider whether the PCA flux modulation is consistent with the proposed period. In Fig. **??** we plot the PCA fluxes on the folded ASM flux with the PCA peak flux arbitrarily normalized. It is seen that the peak PCA flux and decline from this have similar behavior to the folded ASM flux. However, the last few PCA observations fall below the average ASM flux. In Fig. **??** we overplot the PCA fluxes and the smoothed, but not folded, ASM fluxes. There is good overall agreement of the modulation seen in the two instruments. The ASM data suggest that a modest outburst at the time of the next predicted maximum may have occurred shortly after the PCA observations ceased. It thus appears that the light curve obtained with the PCA is consistent with the proposed 61 day modulation.

We note that the *Swift* non-detection of XTE J1859+083 (Romano et al. 2007) occurred at a phase of 0.85. The folded ASM light curve (Fig. **??**) shows that XTE J1859+083 has generally been bright at that phase, suggesting that the source may have been in an extended inactive state. The occurrence of extended inactive states where the outbursts near periastron passage cease is common for Be/neutron star binaries.

4. Conclusion

The spectral, flux variability, and timing properties of XTE J1859+083 appear to be consistent with a Be star X-ray binary classification. Additional observations to further reduce the size of the error box would be valuable, and these should preferably be carried out at the peak of the candidate 60 day period.

We thank Cees Bassa for making the DSS finding charts.

REFERENCES

Charles, P.A., & Coe, M.J. 2006, in Compact Stellar X-ray Sources, ed. W.H.G. Lewin & M. van der Klis (Cambridge: Cambridge Univ. Press), 215

Corbet, R.H.D. 1986, MNRAS, 220, 1047

Corbet, R.H.D., Markwardt, C.B., & Tueller, J. 2007a, ApJ, 655, 458

Corbet, R., Markwardt, C., Barbier, L., Barthelmy, S., Cummings, J., Gehrels, N., Krimm, H., Palmer, D., Sakamoto, T., Sato, T., & Tueller, J. 2007b, proceedings of "The

Extreme Universe in the Suzaku Era", Kyoto, Japan, December 4-8, 2006. Progress of Theoretical Physics Supplement, 169, 200

Jager, R., Mels, W. A., Brinkman, A. C., Galama, M. Y., Goulooze, H., Heise, J., Lowes, P., Muller, J. M., Naber, A., Rook, A., Schuurhof, R., Schuurmans, J. J., & Wiersma, G. 1997, A&AS, 125, 557

Jahoda, K., Swank, J. H., Giles, A. B., Stark, M. J., Strohmayer, T., Zhang, W., & Morgan, E. H. 1996 Proc. SPIE, 2808, 59

Jahoda, K., Markwardt, C. B., Radeva, Y., Rots, A. H., Stark, M. J., Swank, J. H., Strohmayer, T. E., Zhang, W. 2006, ApJS, 163, 401

Joss, P.C., & Rappaport, S. 1984, ARA&A, 22, 537

Levine, A.M., Bradt, N., Cui, W., Jernigan, J.G., Morgan, E.H., Remillard, R., Shirey, R.E., & Smith, D.A. 1996, ApJ, 469, L33

Marshall, F. E., in 't Zand, J. J. M., Strohmayer, T., & Markwardt, C. B. 1999, IAUC 7240

Monet, D.G., et al. 2004, AJ, 125, 984

Romano, P., Mangano, L., Sidoli, V., & Mereghetti, S. 2007, ATEL 1287

Scargle, J.D., 1982, ApJ, 263, 835

Stella, L., White, N.E., & Rosner, R. 1986, ApJ, 308, 669

Verrecchia, F., in't Zand, J. J. M., Giommi, P., Santolamazza, P., Granata, S., Schuurmans, J. J., & Antonelli, L. A. 2007, A&A, 472, 705

White, N.E., Swank, J.J., & Holt, S.S. 1983, ApJ, 270, 711

Table 1. *RXTE* PCA Pointed Observations of XTE J1859+083

Observation ID	Start (MJD)	End (MJD)	Exposure (s)
1	51406.93272	51406.98342	1184
2	51408.23485	51408.33245	4976
3	51409.85825	51409.87297	1072
4	51411.16430	51411.18726	1952
5	51412.16282	51412.18671	1984
6	51413.22880	51413.25615	2144
8	51414.03024	51414.04171	976
7	51414.09300	51414.11300	1568
9	51415.09189	51415.14485	1584
10	51415.17253	51415.18319	912
12	51417.02948	51417.03893	800
11	51417.08985	51417.11022	1584
14	51419.15636	51419.17852	1888
13	51419.22750	51419.25004	1920
16	51420.31178	51420.32995	752
15	51420.38468	51420.39592	832
17	51425.97901	51425.99036	128
18	51426.01698	51426.02911	1040
19	51428.97416	51429.02578	1280
20	51432.23217	51432.24102	768
21	51432.30152	51432.31536	1056
22	51435.87078	51435.91116	1008
23	51439.01763	51439.03967	1808
25	51441.74263	51441.74866	528
24	51441.81208	51441.83269	1744
26	51444.73542	51444.74588	896
27	51444.82212	51444.83272	816

Note. — Start and stop times are not barycenter corrected. Observations are listed in time order which differs from the order of the *RXTE* observation number as parts of proposal number 40137. MJD 51,406 = 1999-08-16

Table 2. *RXTE* PCA Spectral Measurements of XTE J1859+083

Observation ID	2 - 10 keV Flux (ergs cm^{-2} s^{-1})	Flux Lower Limit	Flux Upper Limit	Photon Index	N_H ($10^{22} cm^{-2}$)	E_{cut} (keV)	E_{fold} (keV)	Count Rate	χ^2_ν
1	1.615e-10	1.606e-10	1.625e-10	0.93 ± 0.21	2.98 ± 1.58	6.75 ± 0.36	13.30 ± 0.88	68.02 ± 0.45	0.83
2	1.586e-10	1.581e-10	1.590e-10	0.75 ± 0.11	1.53 ± 0.76	6.39 ± 0.20	13.54 ± 0.52	64.50 ± 0.23	1.06
3	1.439e-10	1.428e-10	1.451e-10	0.76 ± 0.31	0.95 ± 2.32	7.15 ± 0.50	15.07 ± 1.37	41.83 ± 0.39	0.47
4	1.425e-10	1.419e-10	1.432e-10	0.91 ± 0.19	2.54 ± 1.42	6.63 ± 0.30	13.69 ± 0.77	73.93 ± 0.41	0.91
5	1.301e-10	1.295e-10	1.308e-10	0.69 ± 0.16	1.54 ± 0.99	6.05 ± 0.30	12.12 ± 0.78	70.65 ± 0.40	0.77
6	1.255e-10	1.248e-10	1.261e-10	0.95 ± 0.22	2.99 ± 1.52	6.28 ± 0.36	13.37 ± 0.96	50.73 ± 0.33	0.44
8	1.189e-10	1.181e-10	1.200e-10	0.75 ± 0.31	1.72 ± 2.04	6.30 ± 0.50	12.26 ± 1.23	47.43 ± 0.47	1.21
7	1.200e-10	1.193e-10	1.209e-10	0.99 ± 0.27	3.85 ± 1.91	6.29 ± 0.39	12.11 ± 0.95	47.73 ± 0.38	0.80
9	1.070e-10	1.062e-10	1.082e-10	0.97 ± 0.33	2.09 ± 2.40	6.61 ± 0.60	15.92 ± 1.87	29.44 ± 0.31	0.83
10	1.090e-10	1.080e-10	1.099e-10	0.98 ± 0.30	3.04 ± 2.00	6.14 ± 0.51	13.36 ± 1.41	71.33 ± 0.64	0.62
12	9.054e-11	8.906e-11	9.185e-11	0.90 ± 0.47	1.63 ± 3.68	7.00 ± 0.74	13.34 ± 1.89	24.39 ± 0.42	0.90
11	9.370e-11	9.264e-11	9.484e-11	0.73 ± 0.35	0.65 ± 2.42	6.59 ± 0.57	13.61 ± 1.54	25.22 ± 0.30	0.98
14	7.271e-11	7.193e-11	7.341e-11	0.99 ± 0.31	2.93 ± 2.10	6.21 ± 0.48	12.59 ± 1.30	37.37 ± 0.38	1.08
13	7.074e-11	7.005e-11	7.146e-11	1.02 ± 0.33	3.27 ± 2.35	6.25 ± 0.46	12.16 ± 1.19	36.46 ± 0.37	0.92
16	5.338e-11	5.207e-11	5.481e-11	0.95 ± 0.74	2.43 ± 4.88	6.27 ± 0.92	10.73 ± 2.08	20.27 ± 0.49	0.72
15	5.196e-11	5.037e-11	5.347e-11	1.00 ± 0.81	0.89 ± 5.49	6.40 ± 1.37	14.52 ± 4.17	13.73 ± 0.38	0.85
17	1.537e-11	1.146e-11	1.857e-11	1.17 ± 7.20	20.97 ± 52.43	6.45 ± 2.48	3.53 ± 2.58	5.15 ± 1.23	0.56
18	1.645e-11	1.523e-11	1.779e-11	1.42 ± 1.99	3.39 ± 13.01	6.67 ± 2.64	11.82 ± 7.15	5.80 ± 0.42	0.48
19	2.580e-11	2.469e-11	2.692e-11	1.81 ± 0.95	7.94 ± 7.20	6.13 ± 1.03	7.98 ± 1.89	9.40 ± 0.38	0.50
20	3.543e-11	3.391e-11	3.689e-11	0.97 ± 0.81	1.34 ± 4.85	5.76 ± 2.57	17.94 ± 10.26	16.20 ± 0.50	0.53
21	3.490e-11	3.367e-11	3.617e-11	1.15 ± 0.85	3.23 ± 6.21	6.73 ± 2.09	20.41 ± 8.23	17.16 ± 0.43	1.12
22	2.694e-11	2.577e-11	2.818e-11	1.00 ± 1.10	2.52 ± 6.69	6.14 ± 1.43	10.49 ± 3.29	9.37 ± 0.41	0.90
23	1.304e-11	1.198e-11	1.389e-11	1.22 ± 1.84	0.37 ± 11.24	6.44 ± 1.67	9.31 ± 3.49	4.51 ± 0.30	1.01
25	5.117e-12	3.725e-12	6.039e-12	0.56 ± 10.04	0.43 ± 32.94	6.19 ± 3.05	3.96 ± 4.42	2.51 ± 0.66	0.69
24	5.235e-12	4.223e-12	6.120e-12	1.80 ± 3.09	5.67 ± 22.59	6.79 ± 1.02	1.68 ± 1.00	0.67 ± 0.30	0.90
26	5.747e-12	4.502e-12	6.622e-12	2.37 ± 3.94	1.52 ± 20.96	3.65 ± 10.32	9.99 ± 34.44	2.52 ± 0.43	0.73
27	4.731e-12	3.289e-12	5.660e-12	0.89 ± 3.27	0.00 ± 52.25	7.31 ± 1.28	0.73 ± 1.25	-0.58 ± 0.43	1.00

Note. — The flux is not corrected for absorption. Flux upper and lower limits are 1σ confidence intervals obtained from fitting the spectra with all parameters fixed at the mean values from fitting all spectra, with the exception of the normalization and E_{fold}.

Table 3. *RXTE* PCA Pulse Period Measurements of XTE J1859+083

Observation Numbers	Start Time (MJD)	Period (s)
1, 2	51406.93272	9.80098 ± 0.00002
3, 4	51409.85825	9.79773 ± 0.00001
5, 6	51412.16282	9.79819 ± 0.00003
8, 9	51414.03024	9.79716 ± 0.00001
10, 11	51415.17253	9.79526 ± 0.00001
14, 15	51419.15636	9.79532 ± 0.00003
20, 21, 22	51432.23217	9.80170 ± 0.00001

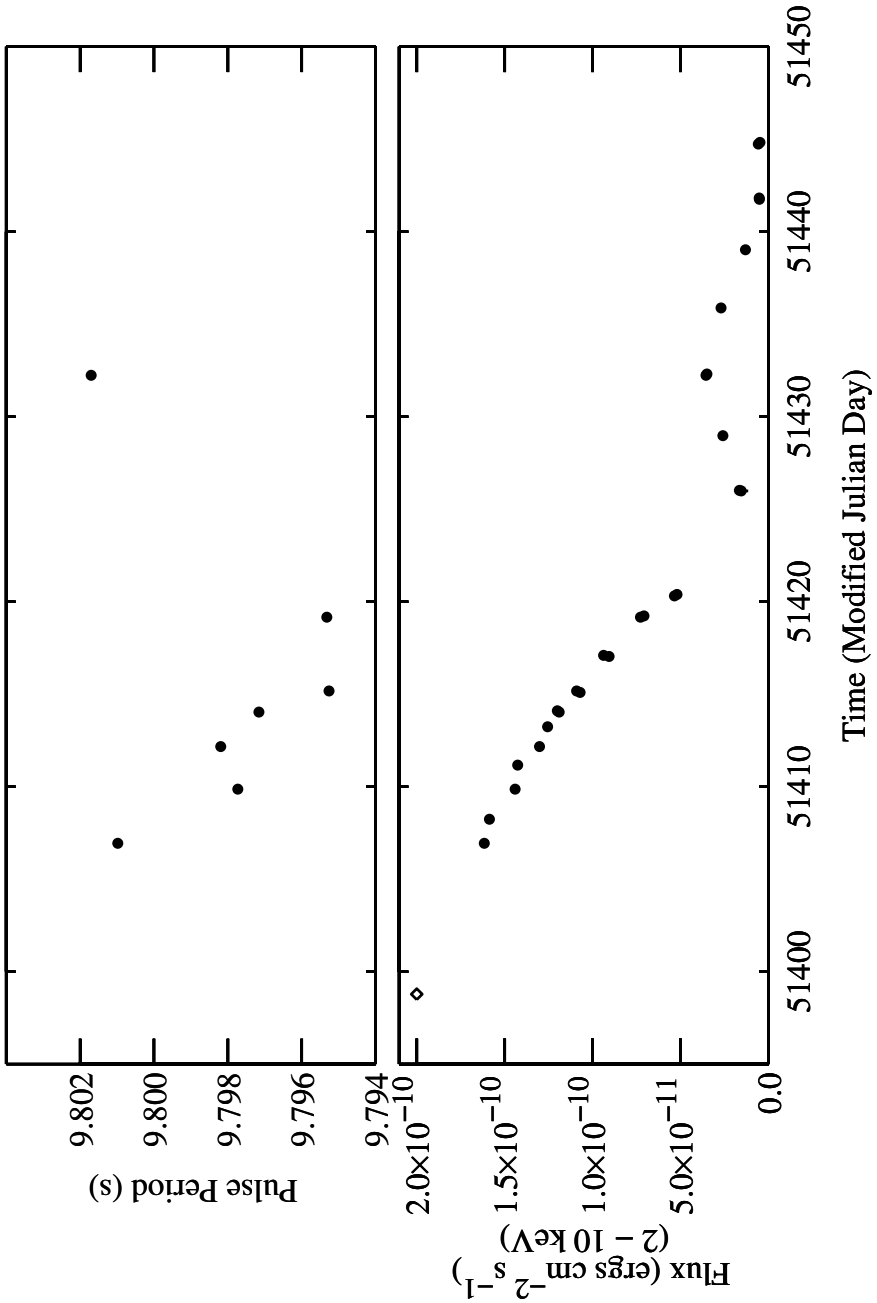

Fig. 1.— *RXTE* PCA measurements of the flux (lower panel) and pulse period (upper panel) of XTE J1859+083. Pulse period measurements were not possible for all observations. Flux and pulse period values are also given in Tables ?? and ?? with the exception of the first flux measurement, marked with a diamond, which is taken from Marshall et al. (1999) and for which no error is available. The errors on the pulse period and flux measurements are smaller than the symbol size.

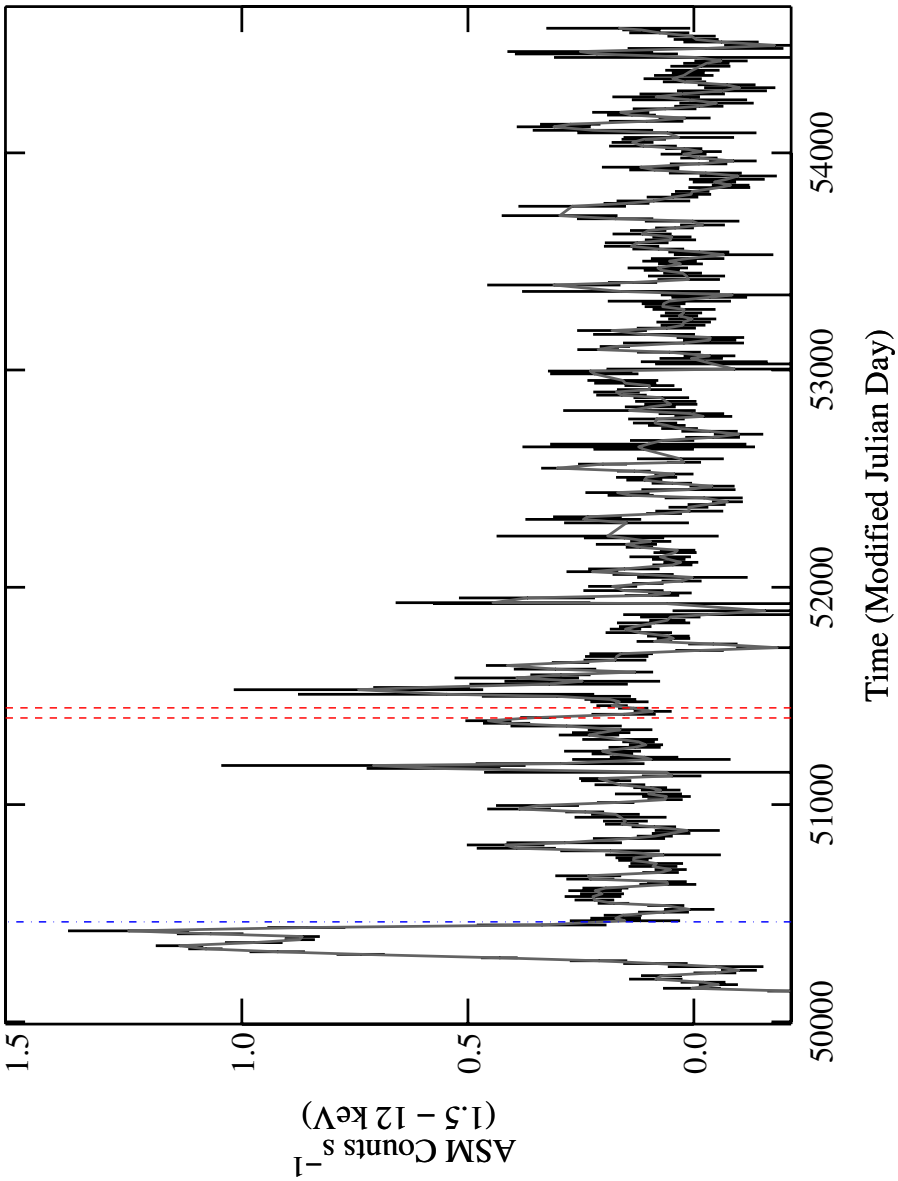

Fig. 2.— The *RXTE* ASM light curve of XTE J1859+083. The light curve has two week time bins which were then smoothed (50% of initial value plus 25% of neighboring points). The red vertical dashed lines indicates the interval during which the PCA observations were made. The vertical dot-dashed blue line indicates MJD 50,460, before which the source may have experienced a "Type II" outburst.

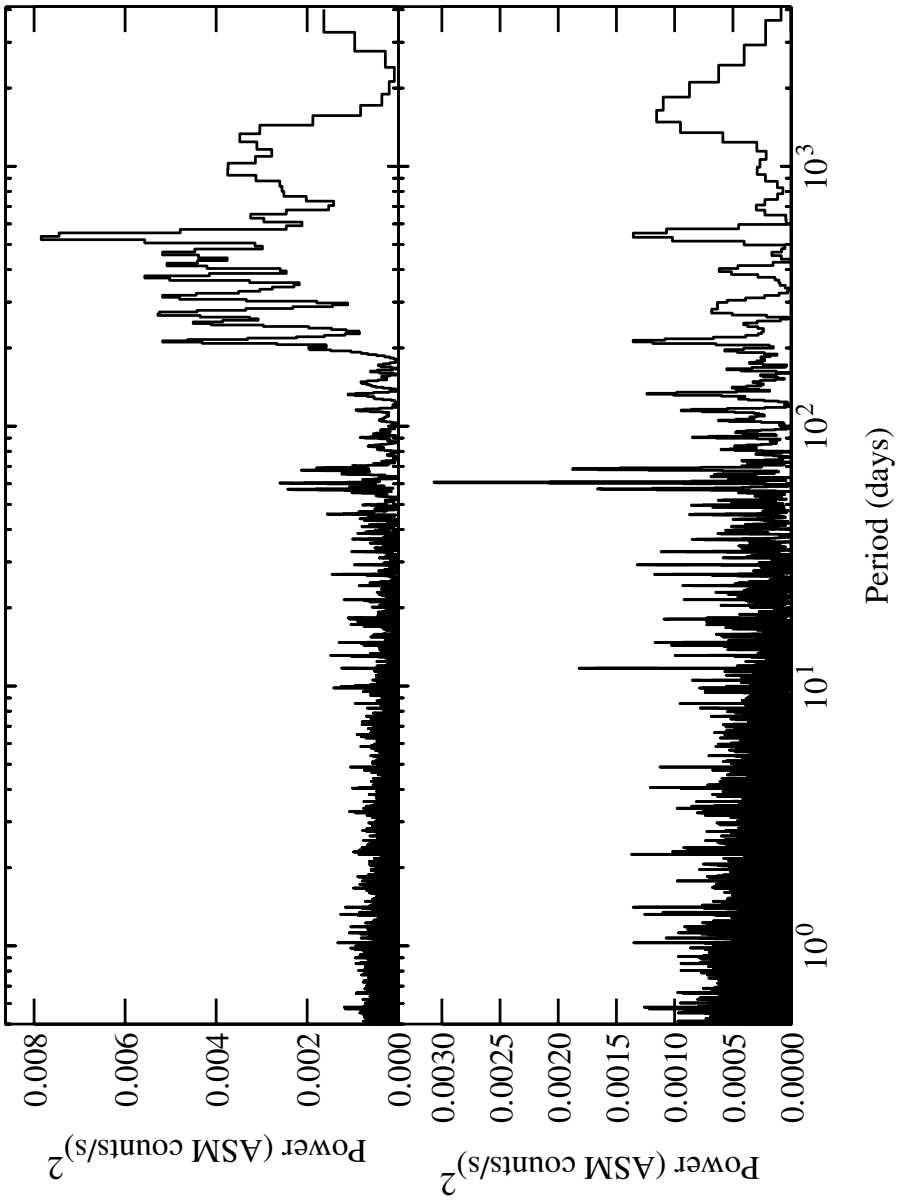

Fig. 3.— Power spectra of the *RXTE* ASM light curve of XTE J1859+083. The upper panel shows the power spectrum of the entire light curve. The lower panel shows the power spectrum using only observations made after MJD 50,460.

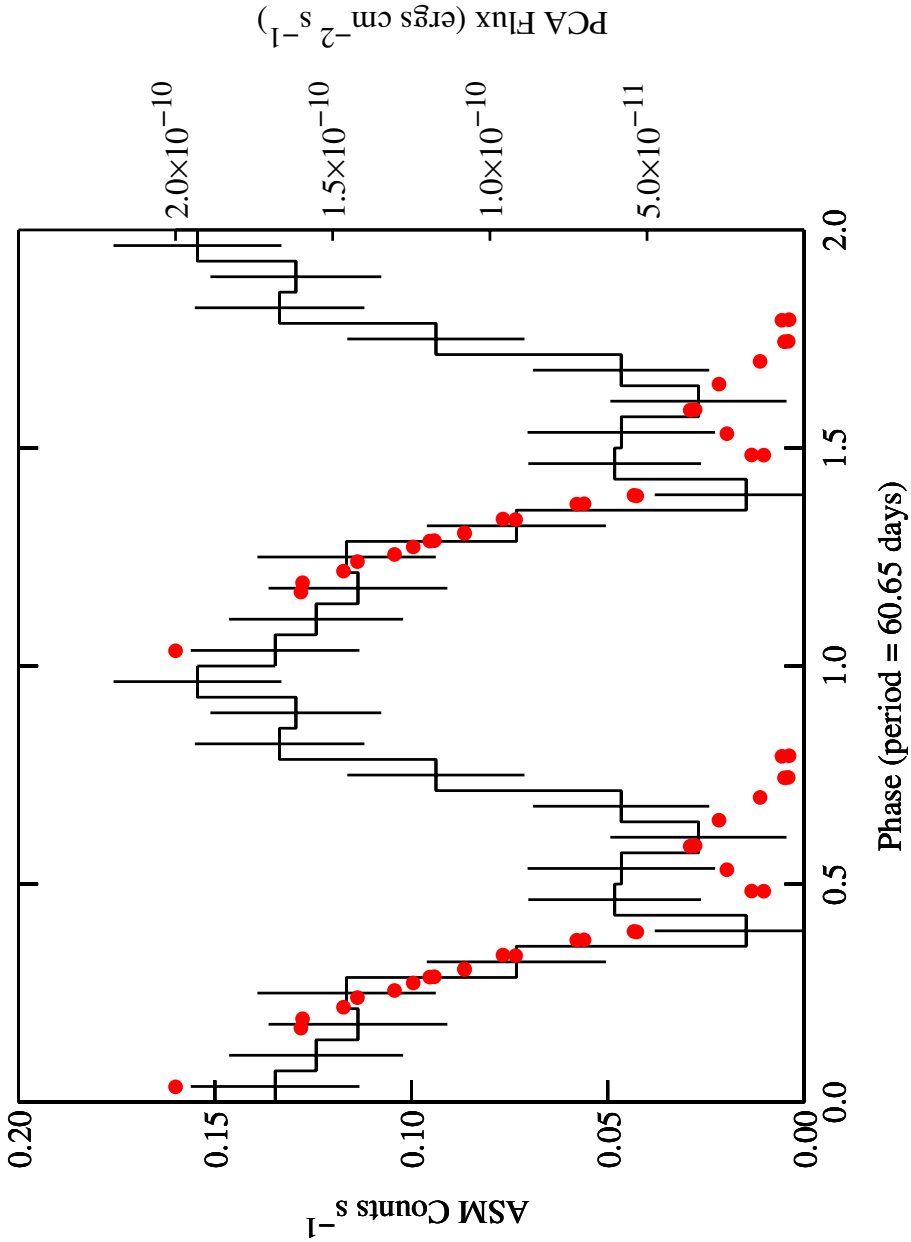

Fig. 4.— *RXTE* ASM light curve of XTE J1859+083 since MJD 50,460 folded on the proposed orbital period (histogram with error bars). The dots show the PCA fluxes scaled to the ASM light curve.

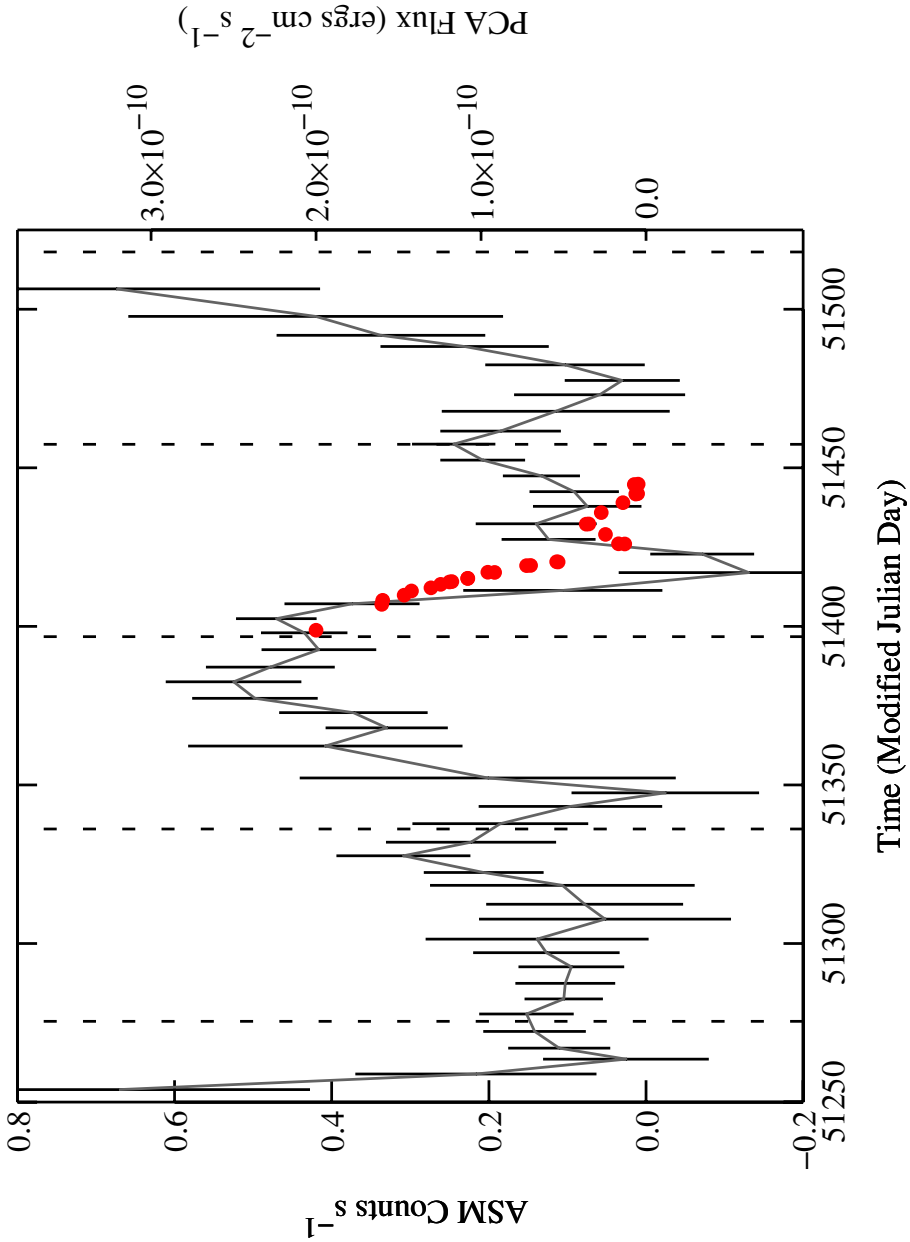

Fig. 5.— ASM light curve of XTE J1859+083 (lines with error bars) around the time when the PCA observations were made. The time resolution is 5 days and the light curve also has been smoothed. The red dots show the PCA fluxes scaled to the ASM light curve. The vertical dashed lines indicate the times of predicted maximum flux based on the possible 60.65 day period.

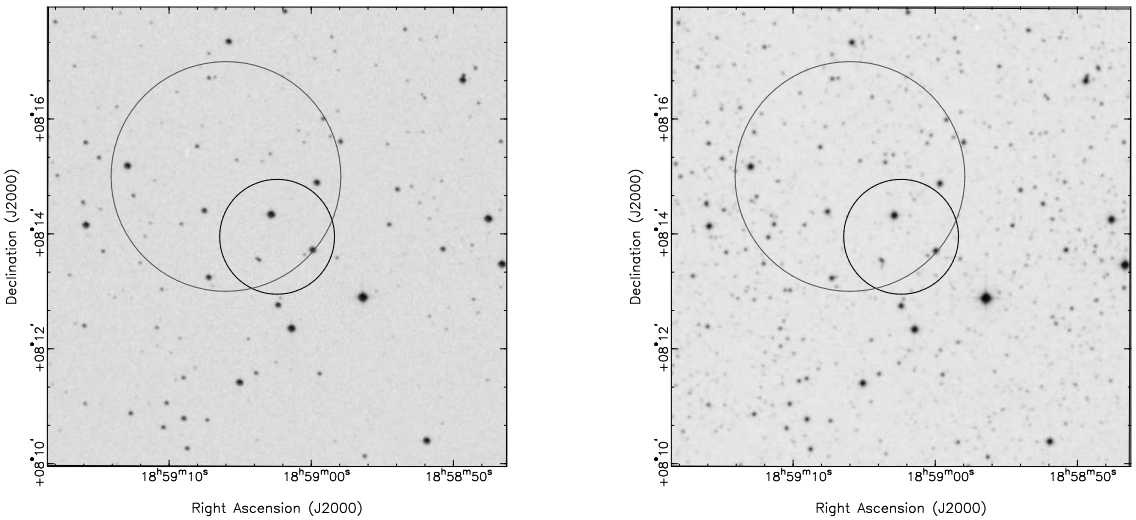

Fig. 6.— Error circles for the position of XTE J1859+083 on Digitized Sky Survey images covering the DSS blue (left) and red (right) bands. North is up and East to the left. The larger error circle to the North East is the *RXTE* PCA error region from Marshall et al. (1999) and the smaller circle is from the *BeppoSAX* WFC observations presented here.